Molecular Pharmacology Fast Forward. Published on March 28, 2007 as doi:10.1124/mol.107.035055

MOL #35055

CCR5 SMALL MOLECULE ANTAGONISTS AND MONOCLONAL ANTIBODIES EXERT POTENT SYNERGISTIC ANTIVIRAL EFFECTS BY CO-BINDING TO THE RECEPTOR

Changhua Ji, Jun Zhang, Marianna Dioszegi, Sophie Chiu, Eileen Rao, Andre deRosier, Nick Cammack, Michael Brandt, and Surya Sankuratri

Department of Viral Diseases (CJ, JZ, MD, ER, AD, NC, SS) and Genome Informatics (SC), Roche Palo Alto, 3431 Hillview Ave., Palo Alto, CA94304.

Pharmaceuticals Division, Roche Penzberg, Penzberg, Germany (MB).

Molecular Pharmacology Fast Forward. Published on March 28, 2007 as DOI: 10.1124/mol.107.035055
This article has not been copyedited and formatted. The final version may differ from this version.

Running Title: Synergy between CCR5 Antagonists and Antibodies

Correspondence should be addressed to: Changhua Ji, Department of Viral Diseases, Roche Palo Alto, 3431 Hillview Ave., Palo Alto, CA94304, Tel. 650 855-6429; Fax. 650 852-1350; Email: Changhua.ji@roche.com

Number of text pages: 32

Number of tables: 4

Number of figures: 9

Number of references: 40

Number of words in abstract: 221

Number of words in introduction: 859

Number of words in discussion: 1272

Abbreviations:

monoclonal antibody (mAb); highly active anti-retroviral therapy (HAART); human immunodeficiency virus (HIV); extracellular loop (ECL); maraviroc (MVC); aplaviroc (APL); vicriviroc (VVC); mean fluorescence intensity (MFI); cell-cell fusion (CCF); combination index (CI); enfuvirtide (ENF); fluorescence-activated cell sorting (FACS); heptad repeat (HR).

Molecular Pharmacology Fast Forward. Published on March 28, 2007 as DOI: 10.1124/mol.107.035055
This article has not been copyedited and formatted. The final version may differ from this version.

ABSTRACT

A panel of four CCR5 mAbs recognizing different epitopes on CCR5 was examined in CCR5-mediated cell-cell fusion assay, alone or in combination with a variety of small molecule CCR5 antagonists. While no antagonism was observed between any of the CCR5 inhibitors, surprisingly potent synergy was observed between CCR5 mAbs and antagonists, and the synergistic activity was confirmed in other antiviral assays. Strong synergy was also observed between CCR5 inhibitors and HIV fusion inhibitor enfuvirtide. There was no synergy observed between small molecule CCR5 inhibitors, however, potent synergy was observed between mAbs recognizing different parts of CCR5. In all synergistic combinations, greater synergy was achieved at higher percent inhibition levels. A negative correlation was found between the degree of synergy between the two classes of CCR5 inhibitors and the ability to compete each other for binding to the receptor. For example, the greatest synergy was observed between mAb ROAb13 and small molecule inhibitor maraviroc which did not interfere with each other's binding to CCR5; while no synergy was found between mAb 45523 and maraviroc which compete for binding to CCR5. In addition, in contrast to a recent report, the CCR5 inhibitors tested here were found to inhibit the same stage of HIV entry. Based on the data presented here we hypothesize that CCR5 inhibitors exert synergistic antiviral actions through a co-binding mechanism.

Molecular Pharmacology Fast Forward. Published on March 28, 2007 as DOI: 10.1124/mol.107.035055
This article has not been copyedited and formatted. The final version may differ from this version.

HAART (highly active anti-retroviral therapy) using three or more anti-human immunodeficiency virus (HIV) agents from different classes in combination has become the standard treatment regime for HIV-infected patients. This treatment strategy has greatly improved the effectiveness of HIV infection control and the survival of acquired immunodeficiency syndrome (AIDS) patients (Barbaro et al., 2005). However, the emergence of drug resistance and drug-related side effects encourages the development of new classes of anti-HIV drugs. One of the most promising steps in the viral life cycle for intervention is the viral entry process. Human immunodeficiency virus (HIV) enters host cells through virus-cell membrane fusion. The first step of viral entry is the high affinity attachment of the HIV envelope protein gp120 to CD4, followed by specific interaction with a chemokine receptor, CCR5 or CXCR4. The CC-chemokine receptor CCR5 is the major coreceptor for HIV and plays a pivotal role in HIV transmission and pathogenesis (Deng et al., 1996; Dragic et al., 1996). CCR5-deficient (Δ32) individuals are essentially protected against infection by HIV-1 in high risk populations. Heterozygous Δ32 individuals are not protected against HIV-1 infection but are often long-term nonprogressors (Eugen-Olsen et al., 1997; Liu et al., 1996). Because it is the predominant coreceptor for the majority of the clinical HIV populations yet appears dispensable for human health, CCR5 has become a very attractive target for anti-HIV therapy.

Many CCR5-targeting small molecules and monoclonal antibodies (mAbs) have been identified in recent years that showed potent anti-viral effect both *in vitro* and *in vivo* (Maeda et al., 2004; Palani et al., 2002; Watson et al., 2005; Wood and Armour, 2005). Recently we also have identified several novel CCR5 monoclonal antibodies (mAb) and small molecule antagonists with potent antiviral activities (Ji et al., 2006a). All known small molecule CCR5 inhibitors are CCR5 antagonists, which bind in the hydrophobic pocket formed by the seven-transmembrane helices. These CCR5 antagonists compete for binding to the same pocket, although they may interact with different residues in the helices (Dragic et al., 2000; Seibert et al., 2006). Because CCR5 antagonists sit deep in the pocket, it is believed that the small

Molecular Pharmacology Fast Forward. Published on March 28, 2007 as DOI: 10.1124/mol.107.035055
This article has not been copyedited and formatted. The final version may differ from this version.

molecule CCR5 antagonists inhibit HIV entry via allosteric mechanism (Watson et al., 2005). Maraviroc is clinically the most advanced CCR5 inhibitor (filed for new drug application in 2007) for HIV therapy, followed by vicriviroc which is in phase 2b/3 trials.

Since HAART is proven to be much more effective than monotherapy, it is important to assess all new anti-HIV agents in development for potential interactions with other antiretroviral drugs. Although *in vitro* drug-drug interactions do not necessarily reproduce *in vivo*, often complicated by pharmacokinetics, it is still necessary to ensure that the new drugs in development do not exert antagonistic interactions with other classes of drugs *in vitro*. Since CCR5 antibodies and small molecule antagonists both target CCR5, it is particularly important to determine if they exhibit any antagonistic interactions in antiviral activities. On the other hand, it would be beneficial if the mAbs and antagonists show synergistic interactions.

When performing drug-drug interaction studies, variable conclusions might be inferred depending on the way data are analyzed. Many models and approaches have been described for the assessment of *in vitro* drug interactions (Chou, 2006; Prichard and Shipman, 1990; Suhnel, 1990). The assumption of no interaction has a central position in these debates, since synergy and antagonism are defined as departures from this. Therefore, when the observed effect is more or less than the effect predicted from the no-interaction theory, synergy or antagonism, respectively, is claimed. Among the various "no-interaction" theories, the Loewe additivity (LA) and Bliss independence (BI) theories are the mostly-referenced models (Greco et al., 1995). The LA theory (Loewe, 1953) is based on the assumption that a drug cannot interact with itself, while the BI theory (SAS-Institute, 1999) is based on the assumption that two drugs act independently with the probabilistic sense of independence. Based on these concepts, various models have been described based on both parametric and nonparametric approaches of these two reference theories. In this study, both the LA-based Greco's model (Greco et al., 1990) and BI-based Prichard's model (Prichard and Shipman, 1990) were used for the analysis of full-range drug-drug interactions between HIV entry inhibitors.

Molecular Pharmacology Fast Forward. Published on March 28, 2007 as DOI: 10.1124/mol.107.035055
This article has not been copyedited and formatted. The final version may differ from this version.

Despite the large numbers of drug combination studies in antiviral assays, there is still heterogeneity regarding the choice of proper assays and data analysis methods. CCR5-mediated cell-cell fusion (CCF) assay is a validated surrogate antiviral assay that yields highly consistent data mainly attributable to the stable effector and target cell lines used in the assay (Ji et al., 2006b). Unlike HIV replication or single-cycle antiviral assays in which the luciferase production takes two or more days to peak, the CCF assay needs only overnight incubation (co-culture) for cell fusion and sufficient luciferase production to be completed. In the current study, several representative CCR5 mAbs and antagonists were tested in the CCF assay, alone and in combinations. Strong synergy was observed between the two novel CCR5 mAbs and CCR5 antagonists. Potent synergistic antiviral effects were also observed between the two novel CCR5 mAbs. In addition, both CCR5 mAbs and antagonists have shown synergistic interactions with the fusion inhibitor enfuvirtide (ENF).

MATERIALS AND METHODS

Reagents. All cell culture media and supplements and fetal bovine sera were purchased from Invitrogen (Carlsbad, CA). Human CCR5 mAb 2D7 and PE-conjugated goat anti-mouse antibodies were purchased from Pharmingen (San Diego, CA). CCR5 mAb 45523 was obtained from R&D Systems (Minneapolis, Minn.). CCR5 antagonists SCH-C (Palani et al., 2002), vicriviroc (VVC, SCH-D) (Strizki et al., 2005), Maraviroc (MVC, UK427,857) (Wood and Armour, 2005), ^{3}H-labeled MVC (^{3}H-MVC), aplaviroc (APL, GW873140, AK602) (Watson et al., 2005), and Roche CCR5 mAbs ROAb13 and ROAb14 (Ji et al., 2006a) and antagonists ROAT-01, ROAT-02, and ROAT-03 were produced in-house. Fusion inhibitor enfuvirtide (ENF, Fuzeon, T20) was obtained from the batches synthesized at Roche for clinical use.

Fluorescence-activated cell sorting (FACS) analysis. CHO-CCR5 cells were harvested and washed twice in phosphate-buffered saline (PBS) containing 0.5% FBS (FACS buffer), then resuspended in FACS buffer at $4x10^6$ cells/ml. For each reaction, 25 µl of cells ($1x10^5$) were transferred to a 5 ml tube

Molecular Pharmacology Fast Forward. Published on March 28, 2007 as DOI: 10.1124/mol.107.035055
This article has not been copyedited and formatted. The final version may differ from this version.

and 1 μg/ml of various primary antibodies and isotype controls were added and the cells were incubated on ice for 30 - 45 min. Cells were washed three times in FACS buffer and incubated with PE-labeled anti-mouse secondary antibodies for 30 min on ice. At the end of incubation, cells were washed 3 times and resuspended in 300 μl of FACS buffer and the stained cells were analyzed with a FACScan Calibur flow cytometer (Becton Dickinson, San Jose, CA)

CCR5-mediated CCF assay. CCF assay was performed as described before (Ji et al., 2006b).

Single-cycle antiviral assay. Pseudotyped NL-Bal viruses were produced by cotransfecting HEK 293T cells with VN1 (HIV pNL4-3 genomic construct with its env gene substituted by a luciferase reporter gene) and pcDNA3.1/NL-BAL *env* [pcDNA3.1 plasmid containing NL-Bal *env* gene (obtained from Roche Welwyn)]. The supernatant containing pseudotyped viruses were stored at -80ºC in aliquots. Reporter cell MAGI-R5 cells were generated by transfecting U373-MAGI-CXCR4CEM cells (Cat.# 3956, NIH AIDS Research & Reference Reagent Program, Germantown, MD) with pcDNA3.1Zeo(-) (Invitrogen, Carlsbad, CA) construct expressing human CCR5 (Ji et al., 2006a). FuGene 6 (Roche Applied Science) was used for the transfection according to manufacturer's instructions. Stable expression population of CCR5 was enriched by 3 rounds of FACS sorting by using PE-labeled 2D7. For the single-cycle HIV entry assay, test antibodies or compounds were serially diluted in 96-well plates. The equivalent of 1.5 x 10^5 RLU of viruses and 2.5 x 10^4 MAGI-R5 cells were added to each well. After 3 day incubation at 37ºC, 50 μl of Steady-Glo Luciferase Assay System was added and the assay plates were read on a Luminometer (Luminsokan, Thermo Electron Corporation, Waltham, MA). Percent inhibition curves were generated using the sigmoidal dose-response model with variable slope in GraphPad PRIZM software (Intuitive Software for Science, San Diego, CA). For the time course study, MAGI-R5 cells ($6x10^4$ /well) were seeded in 24-well plates overnight. HIV-1 pseudotype viruses were chilled at 4°C for 20 minutes and added into pre-chilled MAGI-R5 cells. Spinoculation was performed by spinning at 2000 rpm at 4°C for 1 h. The cells were washed once with cold PBS and then followed by 450 μl of medium at 37°C. At different time points, CCR5 inhibitors at IC_{90} - IC_{95} concentrations were added

Molecular Pharmacology Fast Forward. Published on March 28, 2007 as DOI: 10.1124/mol.107.035055
This article has not been copyedited and formatted. The final version may differ from this version.

to the cells, in 50 μl of medium containing 0.5% FBS. Luciferase activity was measured 48 h post-infection and % virus entry for each time point was calculated as (RLU with inhibitor)/(RLU without inhibitor) x 100.

Radioligand binding assay. Adherent CHO-CCR5 cells at ~90% confluency were detached in freshly-made PBS containing 1 mM ethylenediaminetetraacetic acid (EDTA). Cells were washed twice in PBS without Ca^{2+} and Mg^{2+}, and resuspended in ice cold binding buffer (phenol red-free F12 medium, pH 7.24, supplemented with freshly made 0.1% BSA and 0.1% NaN_3). Cells were then plated in 96-well culture plates at 1.5×10^5 cells/well. Serially diluted CCR5 mAbs were added to the cells, followed by addition of 26 nM of ^{3}H-MVC. After 2 h of incubation at room temperature with gentle shaking, cells were harvested onto GF/C UniFilter plates using cell harvester. UniFilter Packard plates were pretreated with PBS containing 0.3% polyethylenimine and 0.2% BSA for 30 min prior to harvest. Filter plates were washed 5 times with 25 mM HEPES buffer (pH 7.1) containing 500 mM NaCl, 1 mM $CaCl_2$, and 5 mM $MgCl_2$. Plates were dried in 70^{o}C oven for 20 min, and 40 μl scintillation fluid was added and radioactivity was measured using TopCount NXT (PerkinElmer, Shelton, CT). In all experiments, each data point was assayed in duplicate. Curve fitting and subsequent data analysis were carried out using GraphPad PRIZM software (Intuitive Software for Science, San Diego, CA).

Drug interaction analyses. In the cell-cell fusion assay, the possibility of either enhanced or reduced efficacy of one entry inhibitor in combination with another entry inhibitor were analyzed using two different models. These two models followed two different additive drug interaction theories: the Loewe Additivity (LA) theory and the Bliss Independence (BI) theory.

(1) LA-based model. For the drug interaction models based on the LA theory, the concentrations of the drugs in combination are compared to the concentrations of the drugs alone that produce the same effect. The relationship is described by the equation 1: $d_A / D_A + d_B / D_B$, where d_A and d_B are the concentrations of drugs A and B in combination that elicit a certain effect (e.g. 50% inhibition). D_A and D_B are the iso-effective concentrations (e.g. IC_{50}) for each drug alone. The concentration response

Molecular Pharmacology Fast Forward. Published on March 28, 2007 as DOI: 10.1124/mol.107.035055
This article has not been copyedited and formatted. The final version may differ from this version.

surface approach described by Greco et al. (Greco et al., 1990) was used to analyze the data. The fundamental concept from Loewe (Loewe, 1953) underpins this approach. A seven-parameter non-linear model was fit to all experimental data including percent inhibitions calculated from replicates for all concentrations of the two drugs alone and in combination from two 384-well plates. The calculation was based on equation 2:

$$1 = \frac{D_A}{IC_{50A}\left(\frac{E}{Emax - E}\right)^{1/mA}} + \frac{D_B}{IC_{50B}\left(\frac{E}{Emax - E}\right)^{1/mB}} + \alpha\frac{D_A * D_B}{IC_{50A}IC_{50B}\left(\frac{E}{Emax - E}\right)^{0.5(1/mA+1/mB)}}$$

where E_{max} is the maximal response, over background, at 0 drug concentration; IC_{50A} and IC_{50B} are the median inhibitory concentrations of drugs A and B, respectively, that produce 50% of the E_{max}; m_A and m_B are the slopes of concentration response curves for the drugs A and B, respectively; D_A and D_B are the drug concentrations for drugs A and B, respectively, as inputs in the above equation; E is the measured response at the drug concentrations D_A and D_B, as the output; and α is the drug interaction parameter. The above equation was fit to the complete data set from experiment with unweighted lease squares nonlinear regression using SAS program (SAS-Institute, 1999). The estimates of all seven parameters and their associated asymptotic standard errors and 95% confidence intervals were generated to interpret the results. In addition, the R^2, correlation and covariance matrices, and residual plots were checked for goodness of fit for the model.

To interpret the drug interaction from the model fitting, synergy is indicated when the parameter α was positive and its 95% confidence interval did not include 0. Antagonism is indicated when α was negative and its 95% confidence interval did not include 0. Loewe additivity or no interaction is indicated when the 95% confidence interval of α includes 0. Furthermore, the predicted additivity of the drugs combined was calculated by using all estimated parameters of the Greco model, except α that is fixed at 0. The deviance between the predicted response surface and the predicted additive surface is interpreted as percent synergy (positive percentages, if the response surface is above the additive surface),

Molecular Pharmacology Fast Forward. Published on March 28, 2007 as DOI: 10.1124/mol.107.035055
This article has not been copyedited and formatted. The final version may differ from this version.

or percent antagonism (negative percentages, if the response surface is under the additive surface). A three-dimensional graph and a contour plot were generated to examine the magnitude of synergism as well as to determine the range of drug concentrations that produce synergism.

(2) BI-based model. For the drug interaction models based on the BI theory (Bliss, 1939), the estimates of effect of the drugs combined based on the effect of the drugs alone are compared with the observed data from experiment. Its relationship is described by equation 3: Icomb = IA + IB – IA* IB, where Icomb is the predicted percent inhibition of the drugs A and B in combination that have no interaction. IA and IB are the observed percent inhibition of each drug alone. A three-dimensional approach developed by Prichard et al. (Prichard and Shipman, 1990) was used to access the drug interactions. Theoretical additive interactions were calculated from the dose response curves of the individual drugs based on the Bliss Independence equation. For each combination of the two drugs in each plate, the observed percent inhibitions were subtracted from the theoretical additive percent inhibition to reveal greater than expected activities. The resulting surface would appear as a horizontal plane at 0% inhibition above the predicted additive surface if the interactions were merely additive. Any peaks above this plane would be indicative of synergy. Similarly, any depression in the plane would indicate antagonism. The 95% confidence intervals around the experimental dose response surface were used to evaluate the data statistically. The total sum of differences between the observed percent inhibitions and the upper bound of 95% confidence interval of predicted additive percentages is calculated as a statistically significant synergy volume $\sum$Syn. The total sum of differences between the observed percent inhibitions and the lower bound of 95% confidence interval of predicted additive percentages is calculated as a statistically significant antagonism volume $\sum$Ant. In general, the drug interaction is considered weak when the interaction volume is less than 100%. The interaction is considered moderate when the interaction volume is between 100% and 200%. And, the interaction is considered strong when the interaction volume is more than 200%.

For the analysis of drug-drug interaction in the single-cycle assays, Percent inhibition data from 3 independent experiments were averaged and analyzed for mode of interactions by using the

Molecular Pharmacology Fast Forward. Published on March 28, 2007 as DOI: 10.1124/mol.107.035055
This article has not been copyedited and formatted. The final version may differ from this version.

combination index (CI) method as described by Chou and Talalay (Chou and Talalay, 1984). CI analysis is a commonly used tool for characterizing drug-drug-interactions, it provides qualitative information on the nature of drug interaction and the extent of drug interaction. CI was calculated according to equation 4: $CI = (C_{A,x}/IC_{x,A}) + (C_{B,x}/IC_{x,B})$, $C_{A,x}$ and $C_{B,x}$ are the concentrations of drug A and drug B used in combination to achieve *x*% drug effect. $IC_{x,A}$ and $IC_{x,B}$, are the concentrations for single agents to achieve the same effect. CI < 1 indicate synergy, CI = 1 indicate additive effects, and CI > 1 indicate antagonism.

RESULTS

Novel CCR5 mAbs and small molecule antagonists with potent antiviral activities. Two of the mouse anti-human CCR5 mAbs ROAb13 and ROAb14 that have been described before (Ji et al., 2006a) were tested in the CCR5-mediated cell-cell fusion (CCF) assay, along with two other CCR5 mAbs 2D7 and 45523. Three representative CCR5 antagonists discovered at Roche and three known antagonists were also tested in the CCF assay for IC_{50} determinations. As shown in table 1, both novel CCR5 mAbs ROAb13 and ROAb14 showed strong inhibitory effects in the CCF assay, with an IC_{50} of 14 nM and 1.3 nM respectively. MAb 2D7 also showed potent antiviral activity (IC_{50} = 4.3 nM), and mAb 45523 exhibited weaker inhibitory effects on cell-cell fusion (IC_{50} = 23 nM). In contrast, all CCR5 antagonists exhibited low nM or sub-nM IC_{50}s (0.4 - 5 nM) in the CCF assay system.

Strong synergy between CCR5 mAb ROAb14 and antagonist MVC. CCR5 mAbs and CCR5 antagonists were tested in the CCR5-mediated CCF assay in various combinations for the evaluation of potential interactions. CCF assay was chosen as the primary drug-drug interaction tool because it is easy and quick, and has been well validated as an effective surrogate antiviral assay for the evaluation of HIV entry inhibitors especially CCR5 inhibitors (Ji et al., 2006b). In addition, similar drug-drug interaction results were reported in antiviral and CCF assays (Murga et al., 2006). As shown in Fig. 1*A*, seven-point half-log dilutions of mAb ROAb14 and ten-point half-log dilutions of antagonist MVC were tested in the CCF assay, alone or in various dose combinations. The inhibitory effects at each dose point were

Molecular Pharmacology Fast Forward. Published on March 28, 2007 as DOI: 10.1124/mol.107.035055
This article has not been copyedited and formatted. The final version may differ from this version.

calculated and indicated as percent inhibition. A statistically significant synergy exists where the percent inhibition at a fixed concentration of the drugs is greater than the upper bound of 95% confidence interval of the predicted additive % inhibitions of the drugs at the same concentrations dosed alone. This difference, percent synergy, is defined as a synergy indicator based on Bliss Independence theory. Strong synergy is evident between ROAb14 and MVC on cell-cell fusion. For example, when MVC and ROAb14 were added alone both at 0.27 nM, 13% and 12% of inhibition was obtained, respectively. However, when these two drugs were added together at the same concentration, 42% inhibition was observed. This is 19% greater than the predicted additive 23% inhibition (based on the Bliss Independence equation). Furthermore, 16% synergy with 95% confidence was calculated under this dosing combination. Similarly, the percent synergy with 95% confidence was calculated for all checkerboard dosing points and a 3D graph was generated, which suggested a significant synergy at wide dose ranges for both drugs ROAb14 and MVC (Fig. 1*B*). A contour plot was also generated with each section of 10% increment shown in different colors (Fig. 1*C*). The various dose ranges for ROAb14 and MVC to achieve certain percent synergy were identified from this contour plot and summarized in Fig.1*D*. To achieve 20% or greater synergy, the dose ranges for ROAb14 and MVC are 0.09 - 9 nM and 0.06 - 3.1 nM, respectively. The IC_{50} for ROAb14 and MVC alone was measured as 1.3 nM and 0.6 nM, respectively, well within their synergistic dose ranges. The interaction parameter α of the fully parametric Greco's model was positive (24.8 ± 2.8), and the 95% confidence interval did not overlap 0, indicating a statistically significant synergy (Table 2). When the interaction was determined based on Bliss Independence theory using the Prichard's model, a strong synergy was also suggested (Table 2), with a 385% synergy volume (95% ∑SYN). No antagonistic effects were observed.

It can be inferred from Fig. 1*A* that lower doses of the antibody and antagonist in combination were required than they were added alone to achieve the same percent inhibition. For instance, to reach 95% inhibition, 65 nM and 22.2 nM of ROAb14 and MVC, respectively, were required; however, if both drugs were added together, only 0.8 nM of ROAb14 plus 2.47 nM of MVC was required to achieve 96%

Molecular Pharmacology Fast Forward. Published on March 28, 2007 as DOI: 10.1124/mol.107.035055
This article has not been copyedited and formatted. The final version may differ from this version.

inhibition. A reduction of 81-fold in ROAb14 dose or 9.8-fold in MVC dose was observed in this case. In order to obtain information on the dose effects of ROAb14 and MVC in combination at given inhibition levels, isobolograms were generated at 50%, 75%, 90%, and 95% inhibition levels (Fig. 2). A diagonal straight line is expected if only additive effect is observed, and an inward curve toward the low doses indicates synergism and an outward curve indicates antagonism. Significant synergism was observed for ROAb14 and MVC at various inhibition levels. Reduction of 3.3, 5, 10, and 15 folds in the doses normalized by the respective level of potency for the two drugs was obtained at 50%, 75%, 95%, and 95% inhibition levels, respectively.

Strong synergy between CCR5 mAb ROAb13 and antagonist MVC. To examine if the synergy between CCR5 mAb ROAb14 and CCR5 antagonists apply to all CCR5 antibodies, a few other CCR5 mAbs with different recognition sites were then tested in combination with CCR5 antagonists. ROAb13, which binds to the N-terminal end of CCR5 (Zhang et al., 2007), exhibited much greater synergy than ROAb14 when combined with the same CCR5 antagonist MVC (Fig. 3). The 3D graphs generated by using Greco's (Fig. 3A) and Prichard's (Fig. 3*B*) models showed very similar synergy surface, demonstrating 60% or greater synergy could be obtained by dosing ROAb13 with MVC. The α parameter for the ROAb13-MVC combination was calculated using the Greco's model as 662 ± 99 (Table 2), which is much greater than that for the ROAb14-MVC combination (24.8 ± 2.8).

Interaction between other CCR5 mAbs and antagonists. Murine CCR5 mAb 2D7, which is known to bind to the N-terminal half of extracellular loop 2 (ECL2) of CCR5, exhibited weak to moderate synergy in combination with CCR5 antagonist MVC and APL. The α parameters for 2D7-MVC and 2D7-APL combinations were determined as 13.2 and 2.1, respectively by using Greco's model. These values were much smaller than that for the ROAb13-MVC or ROAb14-MVC combinations (Table 2). Another commercially available anti-CCR5 mAb 45523 that was previously shown to bind multiple exodomains of CCR5 was also investigated for its interactions with CCR5 antagonists. As shown in Table 2, the α parameter and $\sum$Syn for 45523-MVC combination were -0.03 and 3, respectively, suggesting no

Molecular Pharmacology Fast Forward. Published on March 28, 2007 as DOI: 10.1124/mol.107.035055
This article has not been copyedited and formatted. The final version may differ from this version.

synergism between 45523 and MVC. It has been demonstrated that CCR5 antagonist APL completely blocked the binding of mAb 45523 (Maeda et al., 2004). In the current study, interactions between mAb 45523 and various CCR5 antagonists including APL were performed. The result revealed that antagonists APL, MVC, and VVC strongly inhibited 45523 binding by 75 - 85% (Fig. 6*A*). These data suggest that the lack of synergy between mAb 45523 and CCR5 antagonists is probably due to the inhibition of 45523 binding by CCR5 antagonists.

Several other CCR5 antagonists including VVC, APL, and novel antagonists ROAT-01, ROAT-02, and ROAT-03, were also tested for their interactions with various antibodies in the CCF assay system. These antagonists are structurally distinct but all exhibited potent antiviral activities. Both Greco's model and Prichard's model were used to analyze the drug interactions for these different combinations and the results were summarized in Table 2. Among all the CCR5 antagonists, APL exhibited the greatest synergy when in combination with ROAb14 or ROAb13, however, it showed weakest synergy with 2D7.

Interaction between CCR5 mAbs. As mentioned above, CCR5 mAbs with different binding epitopes showed different mode of interaction with CCR5 antagonists. Therefore it is possible that antibodies recognizing different parts of CCR5 may interact with each other differently. In the current study, several CCR5 mAbs were tested for their combinational effects on cell-cell fusion. As shown in Fig. 4*A*, strong synergy was observed when ROAb14 (binds to ECL2) (Zhang et al., 2007) was combined with the N-terminal binding mAb ROAb13. However, no synergy was observed when ROAb14 was combined with 2D7 (Fig. 4*B*). Since CCR5 ECL2 is important for both ROAb14 and 2D7 binding, these two antibodies likely to compete for binding to CCR5. And this was confirmed by FACS analysis (Fig. 6*B*). Pre-incubation of CHO-CCR5 cells with 2D7 completely blocked the binding of ROAb14 to cell surface CCR5 receptor, while pre-incubation with ROAb13 had no effect on ROAb14 binding.

No synergy between small molecule CCR5 antagonists. Published literature suggested that all known CCR5 antagonists bind into the same cleft formed by the transmembrane domains of CCR5, as a result these antagonists bind to CCR5 in a competitive manner (Watson et al., 2005). Therefore, no synergy was

Molecular Pharmacology Fast Forward. Published on March 28, 2007 as DOI: 10.1124/mol.107.035055
This article has not been copyedited and formatted. The final version may differ from this version.

expected for the antagonist–antagonist combinations. To prove this hypothesis, three CCR5 antagonists from different structure classes were tested in two-drug combinations in the CCF assay system. As shown in Fig. 4C, no significant synergism or antagonism was observed between antagonists ROAT-01 and ROAT-02 (α= -0.023 ± 0.01). The same result was also observed between antagonist ROAT-02 and APL (α= 0.11 ± 0.06, 3D graph not shown). This observation is consistent with previously published results (Murga et al., 2006).

Strong synergy between fusion inhibitor ENF and CCR5 inhibitors. It has been hypothesized that inhibitors targeting at different steps of HIV entry/fusion process may exert synergistic interactions (Tremblay, 2004). And this has been proven to be true for some HIV entry inhibitors including fusion inhibitor ENF, CCR5 antagonists, CD4 inhibitors, and gp120 inhibitors (Nagashima et al., 2001; Tremblay, 2004; Tremblay et al., 2005). In the current study, we tested interactions between HIV fusion inhibitor ENF and CCR5 mAbs or CCR5 antagonists in the CCR5-mediated CCF assay system. As shown in Table 3, potent synergistic interactions were found between ENF and mAbs or antagonists (Table 3).

CCR5 mAbs and antagonists inhibit the same stage of viral entry. Multiple stages may exist between the binding of gp120 to CCR5 and the initiation of gp41 conformational changes. Published data suggest that CCR5 mAb PA14 and small molecule antagonists may inhibit different stages of HIV entry and this was used to explain the synergy between the two CCR5 inhibitors (Safarian et al., 2006). We would also like to find out whether this is the case for the mAbs and antagonists used in the current study. For this purpose, the single-cycle antiviral assay was used. First we verified the synergy between CCR5 mAb ROAb14 and antagonist MVC in the single-cycle assay (Fig. 5*A*). Due to low throughput of the assay, only the fixed 1:1 ratio combination was performed and combination index (CI) was used to evaluate synergy. At 90% inhibition level, the CI index for ROAb14 and MVC was 0.146; and at 50% inhibition level, the CI index was 0.116. This result indicates strong synergy between the two CCR5 inhibitors (CI < 1 indicates synergy). To determine whether the CCR5 mAbs and antagonists inhibit different stages of

Molecular Pharmacology Fast Forward. Published on March 28, 2007 as DOI: 10.1124/mol.107.035055
This article has not been copyedited and formatted. The final version may differ from this version.

HIV entry, time course experiments were performed. NL-Bal HIV viruses were spinoculated onto MAGI-R5 cells at 4°C and free viruses were washed away. Synchronized HIV infection was triggered by adding medium or inhibitors at 37°C. Inhibitors were then added at different time points afterwards. As shown in Fig. 5*B*, similar time course curves for mAb ROAb14 and 2D7 and small molecule antagonist MVC were observed, suggesting they inhibit the same stage of HIV entry. The time required for half maximal inhibition ($t_{1/2}$) of viral entry for ROAb14, 2D7, and MVC are 6, 8, and 10 min, respectively. The control fusion inhibitor ENF, which inhibit HIV entry at a later stage, showed a much lagged inhibition time course curve ($t_{1/2}$ = 48 min). Published data suggested that mAb PA14 (the murine form of PRO 140) inhibits later stages than CCR5 antagonists, but our data indicate mAb 2D7 and ROAb14 inhibit the same stage as antagonists. This discrepancy could be due to the fact that 2D7 and ROAb14 recognize different epitopes from PA14.

CCR5 mAbs and CCR5 antagonists can co-bind to the receptor. In order to understand the mechanism of the synergy between CCR5 mAbs and CCR5 antagonists, several experiments were performed to investigate the interactions between CCR5 mAbs and CCR5 antagonists at the receptor binding level. When CHO-CCR5 cells were pre-exposed to excess CCR5 antagonist ROAT-02 for 2 h and then to saturating doses of various fluor-labeled CCR5 mAbs ROAb13 or ROAb14, the total binding of these mAbs was found to be the identical to the no antagonist control samples (Fig. 6C). Considering the long off-rate of ROAT-02 ($T_{1/2off}$ ~ 9 h, our unpublished data), the short mAb incubation time (30 min), as well as the presence of excess antagonists during mAb incubation, this result suggests that the mAbs can bind to the antagonist-bound CCR5 as efficiently as to the antagonist-free CCR5. This data thus suggests that CCR5 mAbs and CCR5 antagonists can co-bind to CCR5.

Effects of CCR5 antagonists on CCR5 mAb affinity and on-rate. The dose responses and on-rates of the CCR5 mAbs were then evaluated in the presence and absence of various antagonists. Based on the time course study data shown in Fig. 7, the on-rate and total binding of ROAb13 and ROAb14 were not affected at all by pre-incubation with and continued presence of CCR5 antagonist MVC, APL,

Molecular Pharmacology Fast Forward. Published on March 28, 2007 as DOI: 10.1124/mol.107.035055
This article has not been copyedited and formatted. The final version may differ from this version.

or VVC. However, the total binding of mAb 2D7 was weakly inhibited by pre-incubation of CHO-CCR5 cells with antagonist APL, MVC, and VVC. The on-rate of 2D7 was also slightly slowed down by these antagonists (Fig. 7*C*). The total binding of 45523 was almost completely blocked by the three antagonists mentioned above, with its on-rate significantly reduced (Fig. 7*D*). The binding of mAb 45523 and 2D7 in the presence of CCR5 antagonists were also tested at multiple concentrations. As shown in Fig. 7*E*, mAb 45523 binding was strongly inhibited by MVC, APL and VVC at all doses. And mAb 2D7 binding was weakly inhibited by the three antagonists at most doses (Fig. 7*F*). In both cases, it appears APL exhibited stronger inhibition than VVC and MVC on 2D7 binding. This supports the observation that APL exhibited the weakest synergy with mAb 2D7 among all the antagonists tested (Table 2). In addition, the EC_{50} of 2D7 was not significantly affected by CCR5 antagonists suggesting a non-competition allosteric inhibition.

Effects of CCR5 mAbs on CCR5 antagonist binding. In order to determine if the binding kinetics of CCR5 antagonists were influenced by the synergistic CCR5 antibodies, the binding of ^{3}H-labeled MVC to CHO cell surface CCR5 was measured at various time points by pre-incubating cells with saturating amount (30 μg/ml) of CCR5 mAb 2D7, ROAb13, or ROAb14. Averaged values from three independent experiments were shown in Fig. 8. The binding of MVC was not affected by pre-incubation of CHO-CCR5 cells with ROAb13 at all time points, suggesting that ROAb13 did not change the on-rate or affinity of MVC to CCR5. However, about 38% and 67% inhibition of MVC binding was observed when CHO-CCR5 cells were pre-incubated with ROAb14 or 2D7, respectively.

Molecular Pharmacology Fast Forward. Published on March 28, 2007 as DOI: 10.1124/mol.107.035055
This article has not been copyedited and formatted. The final version may differ from this version.

DISCUSSION

In the current study, strong synergy was observed between CCR5 mAb ROAb14 or ROAb13 and a CCR5 antagonist. Interestingly, the synergy between ROAb13 and antagonists (mean α parameter = 1187.8) was much greater than that between ROAb14 and antagonists (mean α parameter = 36.6) (Table 2). Our previously published data indicate that ROAb13 binds to the N-terminus of CCR5 whereas ROAb14 primarily binds to ECL2 (Zhang et al., 2007). CCR5 mAb PRO 140 has also been found to act synergistically with CCR5 antagonists in inhibiting cell-cell or virus-cell fusion (Murga et al., 2006; Safarian et al., 2006). PRO 140 binds to multiple exodomains of CCR5 with epitopes different from ROAb13, ROAb14, and 2D7 (Trkola et al., 2001). However, CCR5 mAb 2D7 only showed weak synergy with antagonists and mAb 45523 showed no synergy at all with antagonists. Therefore it appears that not all CCR5 mAbs act synergistically with small-molecule antagonists. The reason for the lack of synergy between 45523 and CCR5 antagonists could be due to the strong inhibition of 45523 binding by CCR5 antagonists (Fig. 6A).

Since antibodies and antagonists targeting the same receptor showed strong synergistic interactions in inhibiting viral entry, it is interesting to find out whether antibodies binding to different epitopes can also exert synergistic antiviral actions. Strong synergy was observed between ROAb14 and ROAb13; however, no synergy was observed between ROAb14 and 2D7. Competition binding data indicates that ROAb13 does not compete with ROAb14 for binding, while 2D7 strongly compete with ROAb14 (Fig. 6*B*). These results suggest that antibodies that do not compete for binding to CCR5 may exhibit synergistic interactions, and antibodies that compete for binding may exert additive or antagonistic interactions. This is in agreement with previous findings of synergistical HIV neutralization by mAbs binding to different epitopes on envelope proteins (Laal et al., 1994; Vijh-Warrier et al., 1996), yet additive HIV neutralization by mAbs binding to similar epitopes on gp41 (Zwick et al., 2005). Similarly, CCR5 antagonists also failed to show any synergy in two-drug combinations possibly due to

their competition for the same binding sites on the receptor. In conclusion, it appears that CCR5 inhibitors that do not interfere with each other's binding may exert synergistic antiviral effects. We demonstrated that the observed strong synergy between ROAb14 or ROAb13 and the antagonists is not through enhanced binding of either molecule to the receptor, but rather likely through synergistic interactions after binding to the receptor. We also showed that greater synergy was obtained at higher CCF inhibition levels (Fig. 2) and the synergy between CCR5 mAb and antagonist negatively correlates with binding inhibition of the inhibitor by its partner (Table 4). Based on these observations, we hypothesize that the synergy between CCR5 inhibitors such as an antibody and a small molecule antagonist requires the co-binding of both inhibitors to the receptor. Greater synergy is expected when higher percentage of CCR5 receptors is occupied by both inhibitors. As shown in figure 9, the small molecule antagonists bind to the pocket while the antibodies bind to the surface of CCR5, allowing the co-binding of a CCR5 mAb and a CCR5 small molecule antagonist. Similarly, because the two CCR5 mAbs ROAb13 and ROAb14 bind to different surface areas of CCR5, they do not interfere with each other's binding to CCR5. Under these circumstances, because two different CCR5 inhibitors can bind to CCR5 simultaneously, synergistic antiviral effects were observed. In contrast, because ROAb14 and 2D7 share epitope K171/E172, they compete for binding to CCR5 and no synergy was observed between these two mAbs.

It is not fully understood yet what conformational changes in HIV envelope proteins and chemokine receptors are required for the fusion to occur and how CCR5 antibodies and antagonists inhibit HIV entry. It is hypothesized that CCR5 may exist in multiple conformational states therefore multiple conformational changes may also occur when CCR5 is bound by antibodies or antagonists (Blanpain et al., 2002). Thus the ultimate inhibitory potency of a CCR5 inhibitor is probably dependent on the combined conformational effects. Two different inhibitors such as a mAb and an antagonist could compensate each other on weak inhibitory conformations to result in synergistic inhibition.

Molecular Pharmacology Fast Forward. Published on March 28, 2007 as DOI: 10.1124/mol.107.035055
This article has not been copyedited and formatted. The final version may differ from this version.

ENF, a 36-amino acid peptide mimetic of gp41 heptad repeat (HR) 2 and its downstream region, is the only HIV entry inhibitor on the market (Lazzarin, 2005). ENF is a potent fusion inhibitor which exerts potent antiviral activities by binding to the HR1 trimeric coiled-coil pre-hairpin intermediate. Interaction of gp120 with coreceptor triggers a series of conformational changes and energy transfers. Factors impeding this energy transfer cascade can slow down the fusion kinetics thus increase the exposure time of the pre-hairpin structures to fusion inhibitors. Platt et al. demonstrated that low numbers of surface CCR5 or the presence of CCR5 antagonist TAK-779 greatly reduced HIV fusion kinetics (Platt et al., 2005). This may help explain the strong synergy between ENF and CCR5 inhibitors described in this article.

Synergistic interactions have been found for a variety of drugs, especially antimicrobial, antiviral and anti-tumor drugs. Most of these synergistic drugs target different molecules that belong to the same pathway or different pathway but leading to the same biological outcome. However, synergy between drugs that target the same protein molecule has been demonstrated only for a few drugs. One well-studied example is the synergy between HIV-1 non-nucleotide reverse transcriptase inhibitors (NNRTI) and nucleotide reverse transcriptase inhibitor (NRTI) AZT (Cruchaga et al., 2005). Synergy between antibodies that target the same proteins were also reported but very rare. Friedman reported that two ErbB-2 antibodies that bind to different epitopes exhibited synergy in inducing receptor internalization (Friedman et al., 2005). Synergy has also been detected for neutralization mAbs recognizing different gp120 or gp41 exodomain epitopes. However, the results were controversial and the synergistic effects were moderate (Laal et al., 1994; Vijh-Warrier et al., 1996). Synergistic neutralization has been demonstrated most extensively between mAbs binding to the V3 loop or CD4 binding domain of gp120 (Laal et al., 1994; Vijh-Warrier et al., 1996). The mechanism of the synergy between HIV neutralizing antibodies remains unclear. Synergistic antiviral effects between two mAbs PA12 and 2D7 that bind to the same molecule CCR5 was also reported (Olson et al., 1999). Here we reported highly potent synergy

between two CCR5 mAbs ROAb13 and ROAb14; we also reported potent synergy between CCR5 mAb ROAb13 or ROAb14 and CCR5 antagonists.

In vitro drug-drug interactions have been examined for a variety of HIV entry inhibitors and synergy was found in all combinations between these inhibitors. These inhibitors target at viral and host proteins that are involved in the attachment/fusion process, including gp120 inhibitor PRO542, gp41 inhibitor ENF, CD4 inhibitor CADA, CCR5 mAbs and antagonists. Synergistic interactions between CCR5 inhibitors and HIV reverse transcriptase or protease inhibitors were also reported (Tremblay, 2004; Tremblay et al., 2005). Combination antiviral therapy including a CCR5 mAb would be highly favorable because antibodies use different administration, uptake, and metabolism routes. Combinations between two CCR5 mAbs that do not compete for binding may also be beneficial; however, combinations between two CCR5 antagonists may be unfavorable. Markedly boosted antiviral effects and potential dose reduction may be achieved if a CCR5 mAb and a CCR5 antagonist is co-administered. Since the synergistic CCR5 mAb and antagonist can co-bind to CCR5, another potential benefit of co-administering CCR5 mAbs and antagonists is the raised hurdle for the emergence of HIV-1 mutants resistant to both inhibitors. In addition, since HIV-1 mutants resistant to one of the CCR5 inhibitors are still susceptible to the other class of CCR5 inhibitors (Trkola et al., 2002), co-administration of both classes of CCR5 inhibitors may greatly facilitate the clearance of existing single drug-resistant HIV variants.

Molecular Pharmacology Fast Forward. Published on March 28, 2007 as DOI: 10.1124/mol.107.035055
This article has not been copyedited and formatted. The final version may differ from this version.

ACKNOWLEDGMENTS

The authors would like to acknowledge our medicinal chemists at Roche Palo Alto especially David Rotstein and Chris Melville for providing the CCR5 antagonists, and the HIV biology group for providing the reagents and technical help for the preparation of pseudotyped NL-Bal HIV virus. We would also like to thank NIH AIDS Reagents and Reference Program for providing us with the reagents that were used in this study.

Molecular Pharmacology Fast Forward. Published on March 28, 2007 as DOI: 10.1124/mol.107.035055
This article has not been copyedited and formatted. The final version may differ from this version.

References

Barbaro G, Scozzafava A, Mastrolorenzo A and Supuran CT (2005) Highly active antiretroviral therapy: current state of the art, new agents and their pharmacological interactions useful for improving therapeutic outcome. *Curr Pharm Des* **11**:1805-43.

Blanpain C, Vanderwinden JM, Cihak J, Wittamer V, Le Poul E, Issafras H, Stangassinger M, Vassart G, Marullo S, Schlndorff D, Parmentier M and Mack M (2002) Multiple active states and oligomerization of CCR5 revealed by functional properties of monoclonal antibodies. *Mol Biol Cell* **13**:723-37.

Bliss CI (1939) The toxicity of poisons applied jointly. *Ann. Appl. Biol.* **26**:585-615.

Chou TC (2006) Theoretical basis, experimental design, and computerized simulation of synergism and antagonism in drug combination studies. *Pharmacol Rev* **58**:621-81.

Chou TC and Talalay P (1984) Quantitative analysis of dose-effect relationships: the combined effects of multiple drugs or enzyme inhibitors. *Adv Enzyme Regul* **22**:27-55.

Cruchaga C, Odriozola L, Andreola M, Tarrago-Litvak L and Martinez-Irujo JJ (2005) Inhibition of phosphorolysis catalyzed by HIV-1 reverse transcriptase is responsible for the synergy found in combinations of 3'-azido-3'-deoxythymidine with nonnucleoside inhibitors. *Biochemistry* **44**:3535-46.

Deng H, Liu R, Ellmeier W, Choe S, Unutmaz D, Burkhart M, Di Marzio P, Marmon S, Sutton RE, Hill CM, Davis CB, Peiper SC, Schall TJ, Littman DR and Landau NR (1996) Identification of a major co-receptor for primary isolates of HIV-1. *Nature* **381**:661-6.

Dragic T, Litwin V, Allaway GP, Martin SR, Huang Y, Nagashima KA, Cayanan C, Maddon PJ, Koup RA, Moore JP and Paxton WA (1996) HIV-1 entry into CD4+ cells is mediated by the chemokine receptor CC-CKR-5. *Nature* **381**:667-73.

Dragic T, Trkola A, Thompson DA, Cormier EG, Kajumo FA, Maxwell E, Lin SW, Ying W, Smith SO, Sakmar TP and Moore JP (2000) A binding pocket for a small molecule inhibitor of HIV-1 entry within the transmembrane helices of CCR5. *Proc Natl Acad Sci U S A* **97**:5639-44.

Eugen-Olsen J, Iversen AK, Garred P, Koppelhus U, Pedersen C, Benfield TL, Sorensen AM, Katzenstein T, Dickmeiss E, Gerstoft J, Skinhoj P, Svejgaard A, Nielsen JO and Hofmann B (1997) Heterozygosity for a deletion in the CKR-5 gene leads to prolonged AIDS-free survival and slower CD4 T-cell decline in a cohort of HIV-seropositive individuals. *Aids* **11**:305-10.

Friedman LM, Rinon A, Schechter B, Lyass L, Lavi S, Bacus SS, Sela M and Yarden Y (2005) Synergistic down-regulation of receptor tyrosine kinases by combinations of mAbs: implications for cancer immunotherapy. *Proc Natl Acad Sci U S A* **102**:1915-20.

Greco WR, Bravo G and Parsons JC (1995) The search for synergy: a critical review from a response surface perspective. *Pharmacol Rev* **47**:331-85.

Greco WR, Park HS and Rustum YM (1990) Application of a new approach for the quantitation of drug synergism to the combination of cis-diamminedichloroplatinum and 1-beta-D-arabinofuranosylcytosine. *Cancer Res* **50**:5318-27.

Ji C, Brandt M, Dioszegi M, Jekle A, Schwoerer S, Challand S, Zhang J, Chen Y, Zautke L, Achhammer G, Baehner M, Kroetz S, Heilek-Snyder G, Schumacher R, Cammack N and Sankuratri S (2006a) Novel CCR5 monoclonal antibodies with potent and broad-spectrum anti-HIV activities. *Antiviral Res*. doi:10.1016/j.antiviral.2006.11.003.

Ji C, Zhang J, Cammack N and Sankuratri S (2006b) Development of a novel dual CCR5-dependent and CXCR4-dependent cell-cell fusion assay system with inducible gp160 expression. *J Biomol Screen* **11**:65-74.

Laal S, Burda S, Gorny MK, Karwowska S, Buchbinder A and Zolla-Pazner S (1994) Synergistic neutralization of human immunodeficiency virus type 1 by combinations of human monoclonal antibodies. *J Virol* **68**:4001-8.

Lazzarin A (2005) Enfuvirtide: the first HIV fusion inhibitor. *Expert Opin Pharmacother* **6**:453-64.

Liu R, Paxton WA, Choe S, Ceradini D, Martin SR, Horuk R, MacDonald ME, Stuhlmann H, Koup RA and Landau NR (1996) Homozygous defect in HIV-1 coreceptor accounts for resistance of some multiply-exposed individuals to HIV-1 infection. *Cell* **86**:367-77.

Loewe S (1953) The problem of synergism and antagonism of combined drugs. *Arzneimittelforschung* **3**:285-90.

Maeda K, Nakata H, Koh Y, Miyakawa T, Ogata H, Takaoka Y, Shibayama S, Sagawa K, Fukushima D, Moravek J, Koyanagi Y and Mitsuya H (2004) Spirodiketopiperazine-based CCR5 inhibitor which preserves CC-chemokine/CCR5 interactions and exerts potent activity against R5 human immunodeficiency virus type 1 in vitro. *J Virol* **78**:8654-62.

Murga JD, Franti M, Pevear DC, Maddon PJ and Olson WC (2006) Potent antiviral synergy between monoclonal antibody and small-molecule CCR5 inhibitors of human immunodeficiency virus type 1. *Antimicrob Agents Chemother* **50**:3289-96.

Nagashima KA, Thompson DA, Rosenfield SI, Maddon PJ, Dragic T and Olson WC (2001) Human immunodeficiency virus type 1 entry inhibitors PRO 542 and T-20 are potently synergistic in blocking virus-cell and cell-cell fusion. *J Infect Dis* **183**:1121-5.

Olson WC, Rabut GE, Nagashima KA, Tran DN, Anselma DJ, Monard SP, Segal JP, Thompson DA, Kajumo F, Guo Y, Moore JP, Maddon PJ and Dragic T (1999) Differential inhibition of human immunodeficiency virus type 1 fusion, gp120 binding, and CC-chemokine activity by monoclonal antibodies to CCR5. *J Virol* **73**:4145-55.

Palani A, Shapiro S, Josien H, Bara T, Clader JW, Greenlee WJ, Cox K, Strizki JM and Baroudy BM (2002) Synthesis, SAR, and biological evaluation of oximino-piperidino-piperidine amides. 1. Orally bioavailable CCR5 receptor antagonists with potent anti-HIV activity. *J Med Chem* **45**:3143-60.

Platt EJ, Durnin JP and Kabat D (2005) Kinetic factors control efficiencies of cell entry, efficacies of entry inhibitors, and mechanisms of adaptation of human immunodeficiency virus. *J Virol* **79**:4347-56.

Prichard MN and Shipman C, Jr. (1990) A three-dimensional model to analyze drug-drug interactions. *Antiviral Res* **14**:181-205.

Safarian D, Carnec X, Tsamis F, Kajumo F and Dragic T (2006) An anti-CCR5 monoclonal antibody and small molecule CCR5 antagonists synergize by inhibiting different stages of human immunodeficiency virus type 1 entry. *Virology* **352**:477-84.

SAS-Institute (1999) *SAS users's guide:Statistics*, Cay, North Carolina.

Seibert C, Ying W, Gavrilov S, Tsamis F, Kuhmann SE, Palani A, Tagat JR, Clader JW, McCombie SW, Baroudy BM, Smith SO, Dragic T, Moore JP and Sakmar TP (2006) Interaction of small molecule inhibitors of HIV-1 entry with CCR5. *Virology* **349**:41-54.

Strizki JM, Tremblay C, Xu S, Wojcik L, Wagner N, Gonsiorek W, Hipkin RW, Chou CC, Pugliese-Sivo C, Xiao Y, Tagat JR, Cox K, Priestley T, Sorota S, Huang W, Hirsch M,

Reyes GR and Baroudy BM (2005) Discovery and characterization of vicriviroc (SCH 417690), a CCR5 antagonist with potent activity against human immunodeficiency virus type 1. *Antimicrob Agents Chemother* **49**:4911-9.

Suhnel J (1990) Evaluation of synergism or antagonism for the combined action of antiviral agents. *Antiviral Res* **13**:23-39.

Tremblay C (2004) Effects of HIV-1 entry inhibitors in combination. *Curr Pharm Des* **10**:1861-5.

Tremblay CL, Giguel F, Chou TC, Dong H, Takashima K and Hirsch MS (2005) TAK-652, a novel CCR5 inhibitor, has favourable drug interactions with other antiretrovirals in vitro. *Antivir Ther* **10**:967-8.

Trkola A, Ketas TJ, Nagashima KA, Zhao L, Cilliers T, Morris L, Moore JP, Maddon PJ and Olson WC (2001) Potent, broad-spectrum inhibition of human immunodeficiency virus type 1 by the CCR5 monoclonal antibody PRO 140. *J Virol* **75**:579-88.

Trkola A, Kuhmann SE, Strizki JM, Maxwell E, Ketas T, Morgan T, Pugach P, Xu S, Wojcik L, Tagat J, Palani A, Shapiro S, Clader JW, McCombie S, Reyes GR, Baroudy BM and Moore JP (2002) HIV-1 escape from a small molecule, CCR5-specific entry inhibitor does not involve CXCR4 use. *Proc Natl Acad Sci U S A* **99**:395-400.

Vijh-Warrier S, Pinter A, Honnen WJ and Tilley SA (1996) Synergistic neutralization of human immunodeficiency virus type 1 by a chimpanzee monoclonal antibody against the V2 domain of gp120 in combination with monoclonal antibodies against the V3 loop and the CD4-binding site. *J Virol* **70**:4466-73.

Watson C, Jenkinson S, Kazmierski W and Kenakin T (2005) The CCR5 receptor-based mechanism of action of 873140, a potent allosteric noncompetitive HIV entry inhibitor. *Mol Pharmacol* **67**:1268-82.

Wood A and Armour D (2005) The discovery of the CCR5 receptor antagonist, UK-427,857, a new agent for the treatment of HIV infection and AIDS. *Prog Med Chem* **43**:239-71.

Zhang J, Rao E, Dioszegi M, Kondru R, Derosier A, Chan E, Schwoerer S, Cammack N, Brandt M, Sankuratri S and Ji C (2007) The Second Extracellular Loop of CCR5 Contains the Dominant Epitopes for Highly Potent Anti-HIV Monoclonal Antibodies. *Antimicrob Agents Chemother*. doi:10.1128/AAC.01302-06.

Zwick MB, Jensen R, Church S, Wang M, Stiegler G, Kunert R, Katinger H and Burton DR (2005) Anti-human immunodeficiency virus type 1 (HIV-1) antibodies 2F5 and 4E10 require surprisingly few crucial residues in the membrane-proximal external region of glycoprotein gp41 to neutralize HIV-1. *J Virol* **79**:1252-61.

Molecular Pharmacology Fast Forward. Published on March 28, 2007 as DOI: 10.1124/mol.107.035055
This article has not been copyedited and formatted. The final version may differ from this version.

FIGURE LEGENDS

Fig. 1. Synergistic interactions between ROAb14 and MVC in inhibiting cell-cell fusion. **A**, CCR5 antagonist MVC and mAb ROAb14 were serially diluted starting from 200 nM and 65 nM respectively. Various doses of both inhibitors were added to the CCR5-mediated CCF assay either alone or in combinations, and percent inhibition of CCF was calculated for various doses of inhibitors. Cells with a value of less than 50% inhibition are shaded for easier identification of synergy. **B**, Three-dimensional dose response surface graph. The doses of both inhibitors were plotted against percent synergy calculated from percent inhibition data shown in A by using Greco model. Percent synergy at each 10% increment is shown in different colors. **C**, All percent synergy levels identified in the 3D graph are plotted in the 2D contour graph, and their corresponding dose ranges for CCR5 mAb and antagonists are listed in table below the contour (**D**). Data are from a representative experiment.

Fig. 2. Isobolograms of ROAb14-MVC combination. Isobolograms were created as described in Method at 50% (**A**), 75% (**B**), 90% (**C**), and 95% (**D**) inhibition levels. X-axis and Y-axis are fractions of 1 unit of percent inhibition concentrations (IC) for ROAb14 and MVC, respectively. Diagonal straight line indicates theoretical additive interactions and the curve under it or above it indicate synergistic or antagonistic interactions between the two drugs (shown in **A**). Fold synergy are indicated in parenthesis for each percent inhibition level.

Fig. 3. Three-dimensional drug response surface for the ROAb13-MVC combinations. Percent synergy obtained from each combination dose was plotted against ROAb13 and MVC doses, based on Greco's (**A**) and Prichard's (**B**) mathematics models.

Molecular Pharmacology Fast Forward. Published on March 28, 2007 as DOI: 10.1124/mol.107.035055
This article has not been copyedited and formatted. The final version may differ from this version.

Fig. 4. In vitro drug interactions between CCR5 mAbs or antagonists. 3D drug response surface graphs for ROAb14-ROAb13 (**A**), ROAb14-2D7 (**B**), and ROAT-01 and ROAT-02 (**C**) combinations were created based on Greco's model.

Fig. 5. CCR5 mAb and antagonist MVC inhibit the same entry stage. **A**, Serially diluted ROAb14 and MVC were added to the single-cycle antiviral assays, alone or in combination at 1:1 ratio. Percent inhibition curves were generated using data from 3 independent experiments. **B**, NL-Bal pseudoviruses were spun onto MAGI-R5 cells at 4ºC. After washing, cells were warmed to 37ºC, and inhibitors were added at different time points. Percent virus entry time course curves were plotted and $t_{1/2}$ values were calculated using one- phase exponential association curve fitting. Data are means of three independent experiments.

Fig. 6. Effects of CCR5 mAb or antagonists on CCR5 mAb binding. **A**, CHO-CCR5 cells were pre-incubated with 50 nM of APL, MVC, VVC, or vehicle at room temperature for 1 h, then incubated with fluor-labeled 45523 on ice for 30 min, followed by FACS analysis. Mean fluorescence intensity (MFI) for each treatment was obtained and converted to percent binding by setting vehicle control MFI as 100%. **B**, CHO-CCR5 cells were pre-incubated with 10 μg/ml of 2D7 or ROAb13 on ice for 1 h, then incubated with fluoro-labeled ROAb14 for 30 min, followed by FACS analysis. MFI for each treatment was obtained and converted to percent binding by setting vehicle control MFI as 100%. Bars with standard errors for panels **A** and **B** are percent mAb binding data from two or more experiments. **C**, CHO-CCR5 cells were pre-incubated with 5 μM of ROAT-02 or vehicle at room temperature for 1 h, then with 1 μg/ml of fluor-labeled ROAb14 or ROAb13 on ice for 30 min in the presence of ROAT-02, followed by FACS analysis. Bars with standard errors are MFI from two independent experiments.

Molecular Pharmacology Fast Forward. Published on March 28, 2007 as DOI: 10.1124/mol.107.035055
This article has not been copyedited and formatted. The final version may differ from this version.

Fig. 7. Effects of CCR5 antagonists on CCR5 mAb binding. (**A**-**D**) time course. CHO-CCR5 cells were pre-incubated with 50 nM of APL, MVC, VVC, or vehicle at room temperature for 1 h, then incubated with fluor-labeled CCR5 mAb ROAb14 (**A**), ROAb13 (**B**), 2D7 (**C**), or 45523 (**D**) on ice for various time points, followed by cell fixation in 2% paraformaldehyde and FACS analysis; or incubated with various doses of fluorescence-labeled CCR5 mAb 45523 (**E**) or 2D7 (**F**) on ice for 30 min, followed by FACS analysis. The time course and dose response curves for each mAb in the presence of various antagonists were created based on their MFI values.

Fig. 8. Effects of CCR5 mAbs on MVC binding. CHO-CCR5 cells ($2x10^5$/100 μl) were pre-incubated with 30 μg/ml of various CCR5 mAbs or PBS at room temperature for 1 h, then incubated with 26 nM of ^{3}H-MVC. At the end of various time points, cells were washed and the membrane-bound ^{3}H-MVC was measured as described in Methods. The maximal counts from the control samples were set as 100% binding and the relative binding for all other samples were calculated and the time course curves were generated based on these relative binding at each time point.

Fig. 9. Diagram of CCR5 structure. CCR5 is a seven-transmembrane protein that contains four extracellular domains: the N-terminal end (black), extracellular loop (ECL) 1, 2, and 3 (green); seven transmembrane helices (pink); and four intracellular domains: the C-terminal end and intracellular loop (ICL) 1, 2, and 3 (purple). The epitopes for CCR5 mAbs 2D7, ROAb13, and ROAb14 (Zhang et al., 2007) are shown. The epitope for 2D7 is K172/E172 (red) in ECL2, the epitope for ROAb14 is K171/E172 (red) and W190 (brown) in ECL2, and the epitope for ROAb13 is the N-terminal eight amino acid residues (blue). The structure of CCR5 antagonist maraviroc (Wood and Armour, 2005) is also shown. Maraviroc binds to the hydrophobic pocket formed by the transmembrane helices.

Molecular Pharmacology Fast Forward. Published on March 28, 2007 as DOI: 10.1124/mol.107.035055
This article has not been copyedited and formatted. The final version may differ from this version.

Table 1. Potency of CCR5 inhibitors in CCF assay

Inhibitor	*Class*	*IC_{50} (mean ± SD, nM)*
ROAT-01	Antagonist	2.1 ± 0.5
ROAT-02	Antagonist	4.2 ± 1.2
ROAT-03	Antagonist	0.4 ± 0.2
VVC	Antagonist	2.5 ± 1.3
MVC	Antagonist	0.6 ± 0.4
APL	Antagonist	0.5 ± 0.3
2D7	mAb	4.3 ± 1.6
45523	mAb	23.0 ± 6.7
ROAb13	mAb	14.0 ± 3.7
ROAb14	mAb	1.3 ± 0.4

Data were from three independent experiments

Molecular Pharmacology Fast Forward. Published on March 28, 2007 as DOI: 10.1124/mol.107.035055
This article has not been copyedited and formatted. The final version may differ from this version.

Table 2. Interaction between CCR5 mAbs and antagonists

Drug 1	Drug 2	Greco Model	Prichard Model	
		α ± SE	∑SYN	∑ANT
ROAb14	APL	126.9 ± 58.8	769	-2
	MVC	24.8 ± 2.8	385	-17
	VVC	20.6 ± 1.7	308	-11
	ROAT-01	20.7 ± 2.6	398	-17
	ROAT-02	16.7 ± 3.1	286	-7
	ROAT-03	9.8 ± 1.8	165	-5
	Median	*36.6*	*385.2*	*-9.8*
ROAb13	APL	3296.3 ± 1113.2	1612	0
	MVC	662.3 ± 99.5	1314	-1
	VVC	555.2 ± 87.0	1164	-3
	ROAT-01	183.6 ± 24.6	995	-8
	ROAT-02	2214.2 ± 568.9	2034	-5
	ROAT-03	215.3 ± 61.6	1144	0
	Median	*1187.8*	*1377.2*	*-3*
2D7	MVC	13.2 ± 1.5	298	-1
	APL	2.1 ± 0.6	113	-1
	ROAT-03	0.3 ± 0.2	45	-36
	Median	*5.2*	*152*	*-16.7*
45523	MVC	-0.03 ± 0.008	3	-102
	APL	-0.03 ± 0.007	2	-114
	Median	*-0.03*	*2.5*	*-108*

Data were from two or more independent experiments

Molecular Pharmacology Fast Forward. Published on March 28, 2007 as DOI: 10.1124/mol.107.035055
This article has not been copyedited and formatted. The final version may differ from this version.

Table 3. Interaction between ENF and CCR5 inhibitors

Drug 1	Drug 2	Greco Model	Prichard Model	
		α ± SE	∑SYN	∑ANT
ENF	ROAb14	32.3 ± 5.4	529	-7
ENF	ROAb13	15.8 ± 2.5	573	-8
ENF	2D7	17.0 ± 5.0	246	0
ENF	MVC	5.8 ± 2.4	96	-9
ENF	ROAT-01	13.7 ± 2.1	192.6	-1.5
ENF	ROAT-02	12.3 ± 3.2	204	-1
ENF	ROAT-03	11.3 ± 1.6	147.5	-1.3
Median		*15.5*	*284*	*-4.0*

Data were from two or more independent experiments

Molecular Pharmacology Fast Forward. Published on March 28, 2007 as DOI: 10.1124/mol.107.035055
This article has not been copyedited and formatted. The final version may differ from this version.

Table 4. Relationship between synergy and binding

Combination	Synergy	% Inhibition*	
	α Parameter	MVC binding	Ab Binding
ROAb13 + MVC	662.3 ± 99.5	0	0
ROAb14 + MVC	25 ± 2.8	38	0
2D7 + MVC	13.2 ± 1.5	67	18
45523 + MVC	0	UD**	80

* % inhibition of the binding of one inhibitor by the partner;

** undetermined

Figure 1

(A)

ROAb14 (nM) \ Maraviroc (nM)	200	66.67	22.22	7.41	2.47	0.82	0.27	0.09	0.03	0.01	0	0
65	97%	97%	97%	97%	97%	97%	97%	97%	96%	96%	95%	95%
21.67	97%	97%	97%	97%	97%	97%	96%	95%	92%	90%	88%	84%
7.22	97%	97%	96%	97%	97%	97%	93%	84%	79%	77%	67%	68%
2.41	97%	97%	97%	97%	97%	94%	83%	68%	62%	52%	48%	41%
0.80	97%	97%	97%	97%	96%	89%	69%	54%	47%	34%	24%	28%
0.27	96%	96%	97%	96%	90%	72%	42%	30%	25%	13%	15%	9%
0.09	96%	97%	96%	93%	79%	57%	16%	10%	7%	9%	8%	5%
0	96%	96%	95%	87%	66%	41%	13%	7%	4%	3%	0%	-1%

(B)

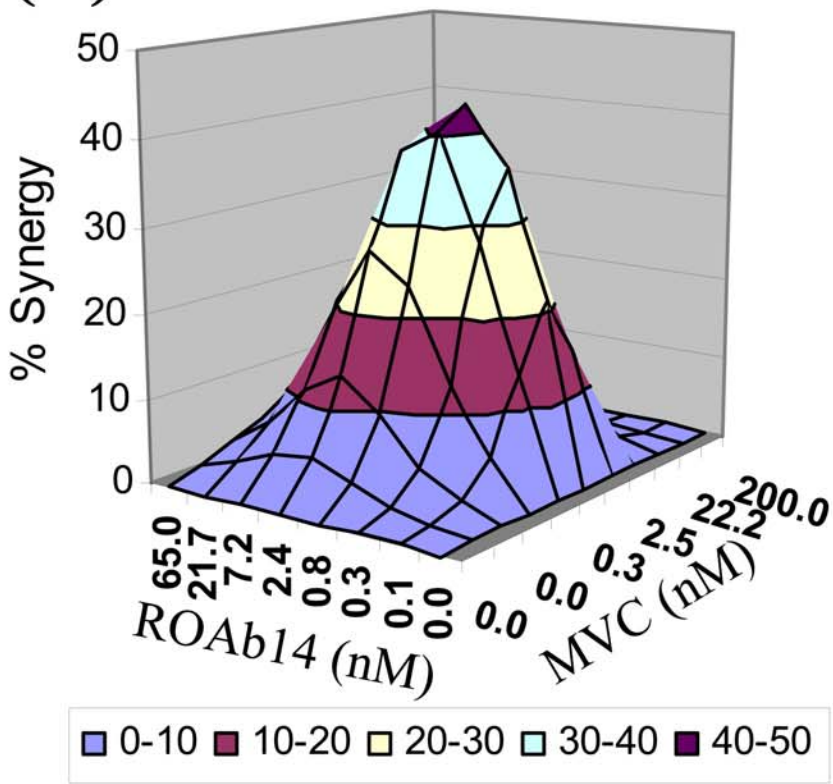

(C)

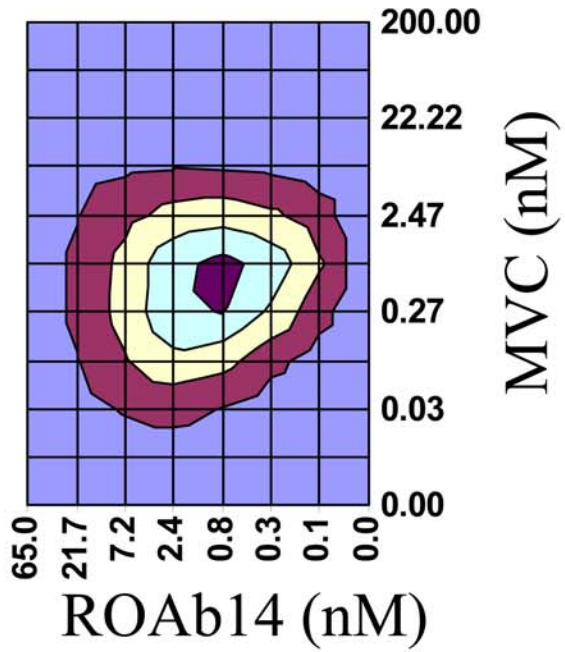

(D)

Dose synergy relationship

Synergy (%)	Dose Range (nM)	
	ROAb14	MVC
10 - 20	0.03 - 26	0.02 - 7
20 - 30	0.09 - 9	0.06 - 3.1
30 - 40	0.2 - 5	0.14 - 1.6
40 - 50	0.6 - 2.5	0.27 - 1

Figure 2

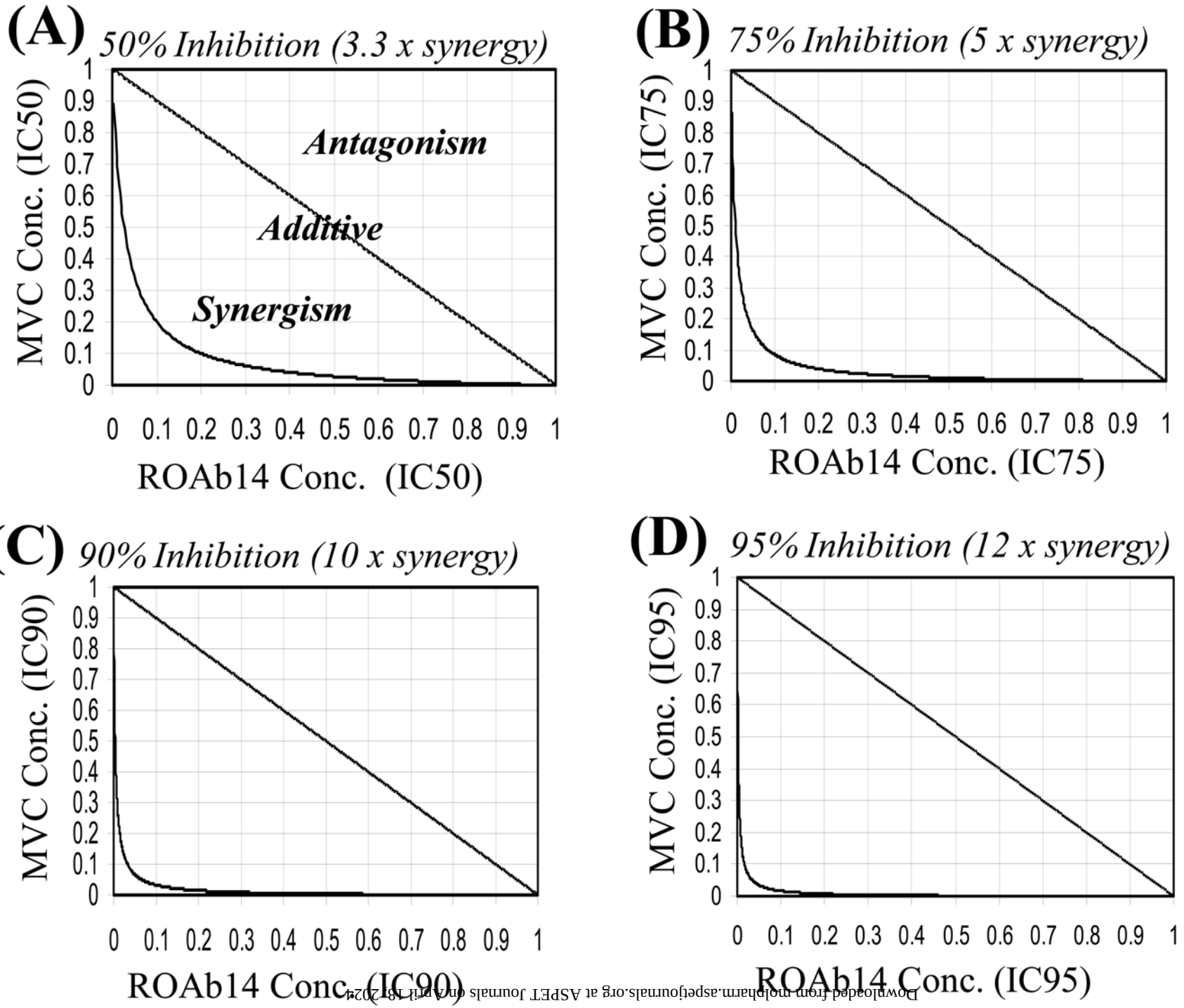

Figure 3

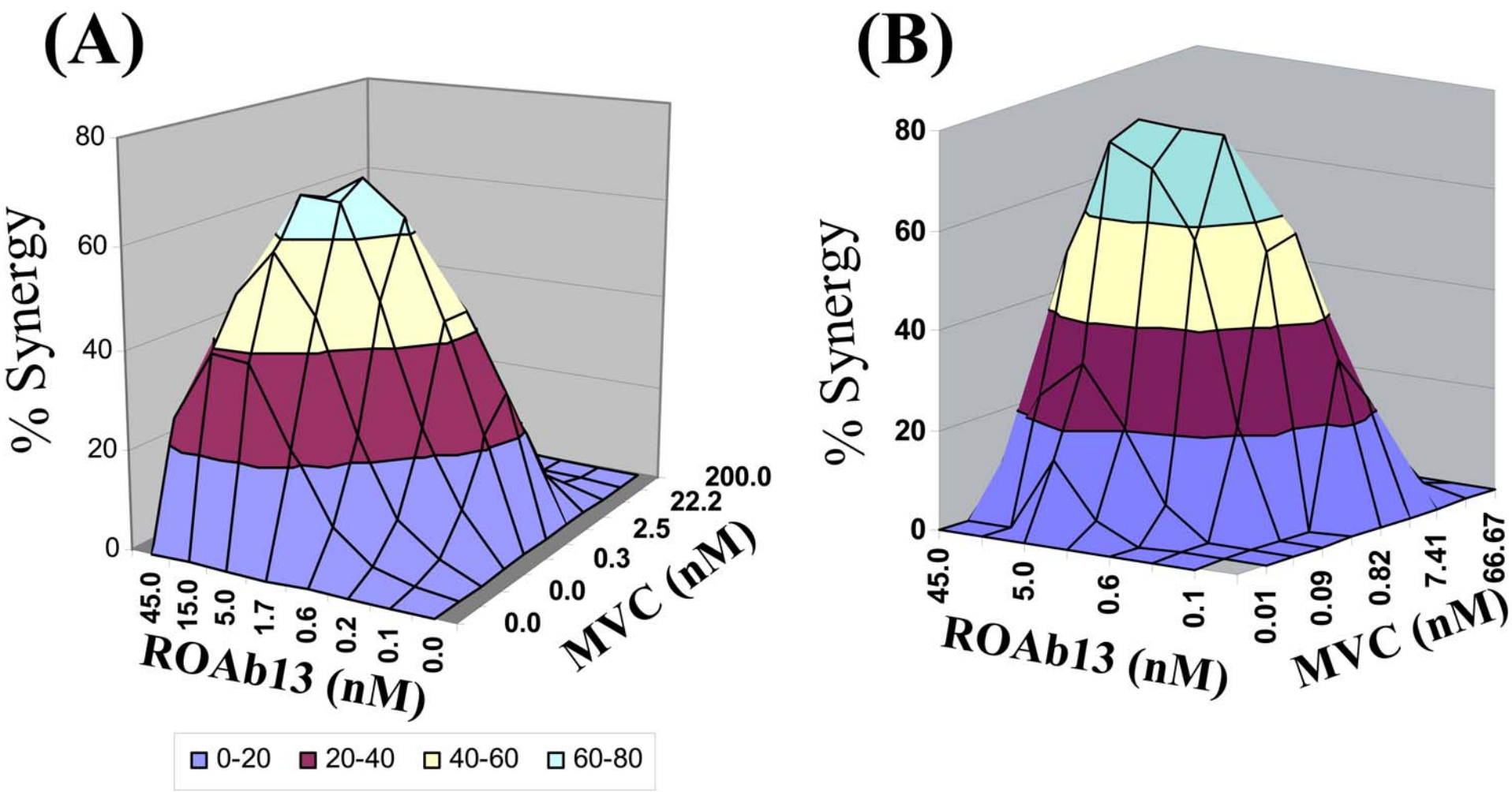

Figure 4

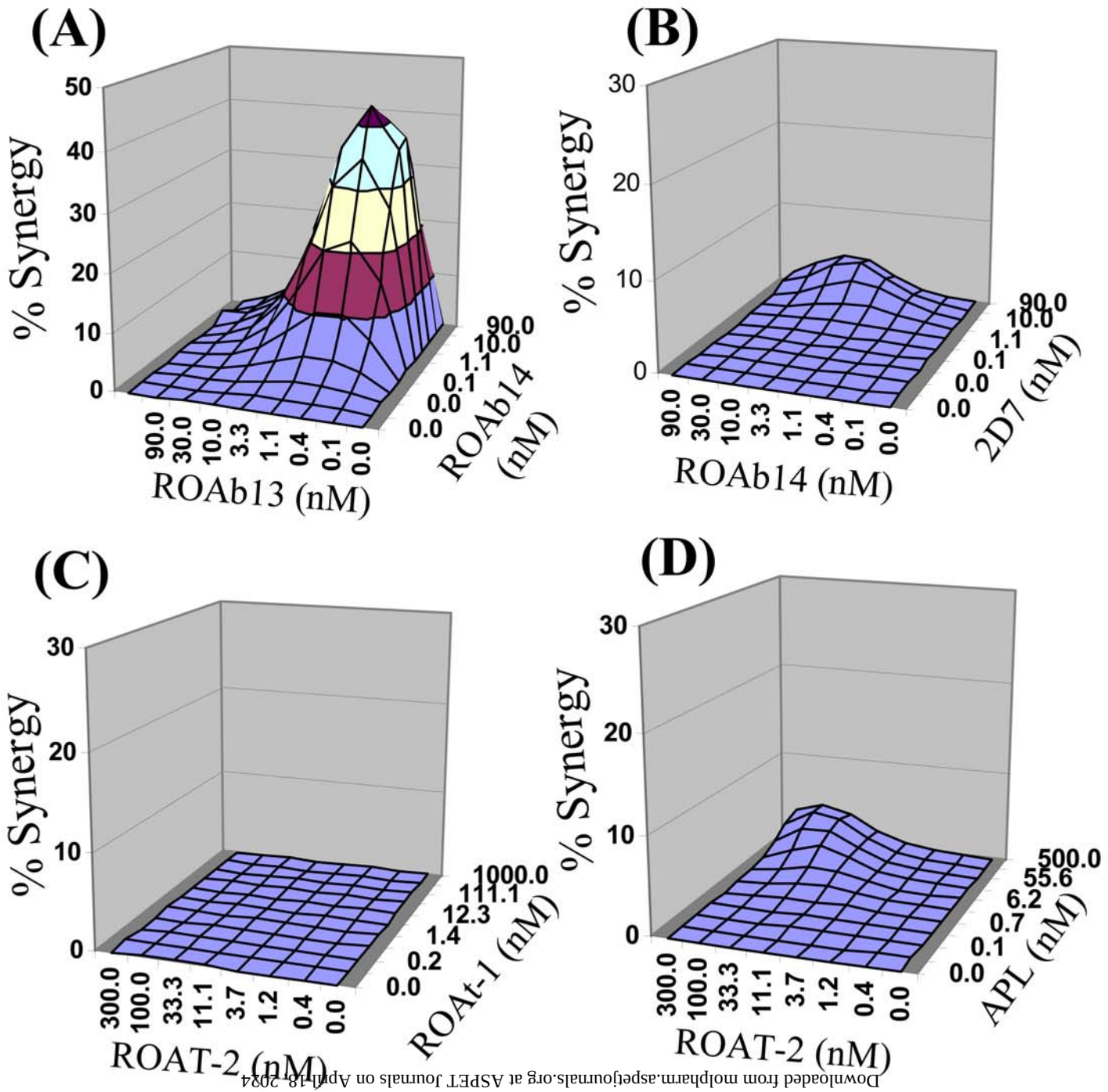

Figure 5

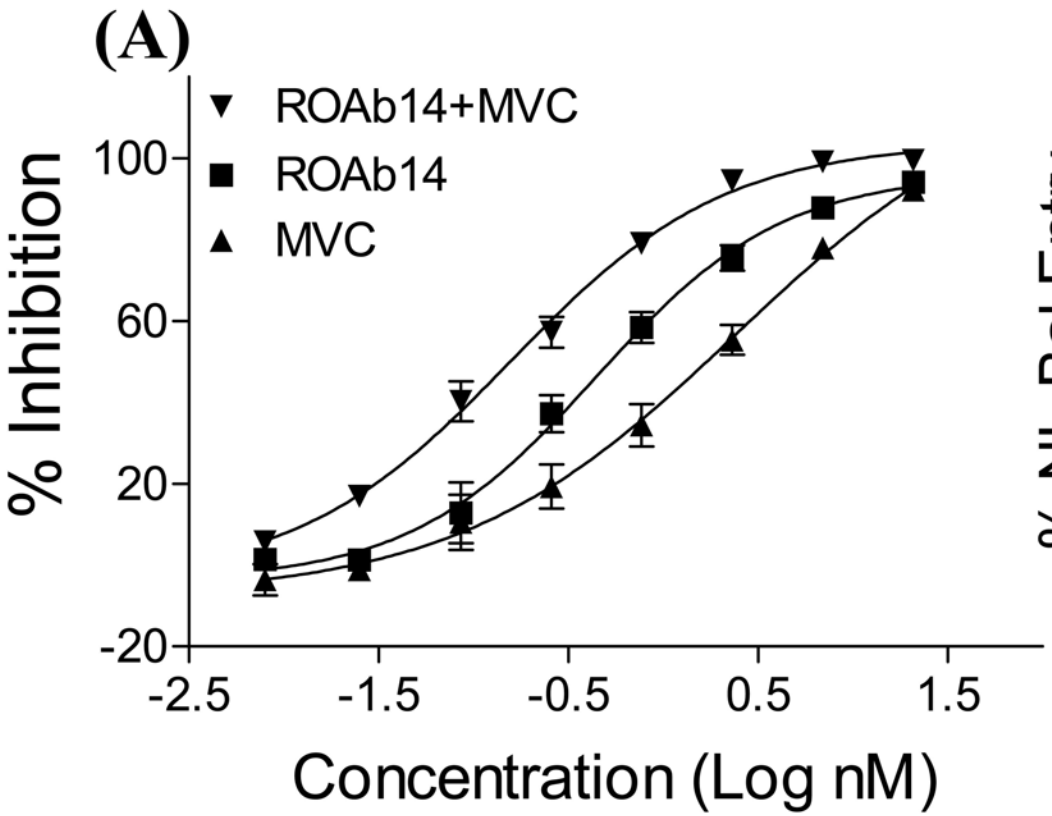

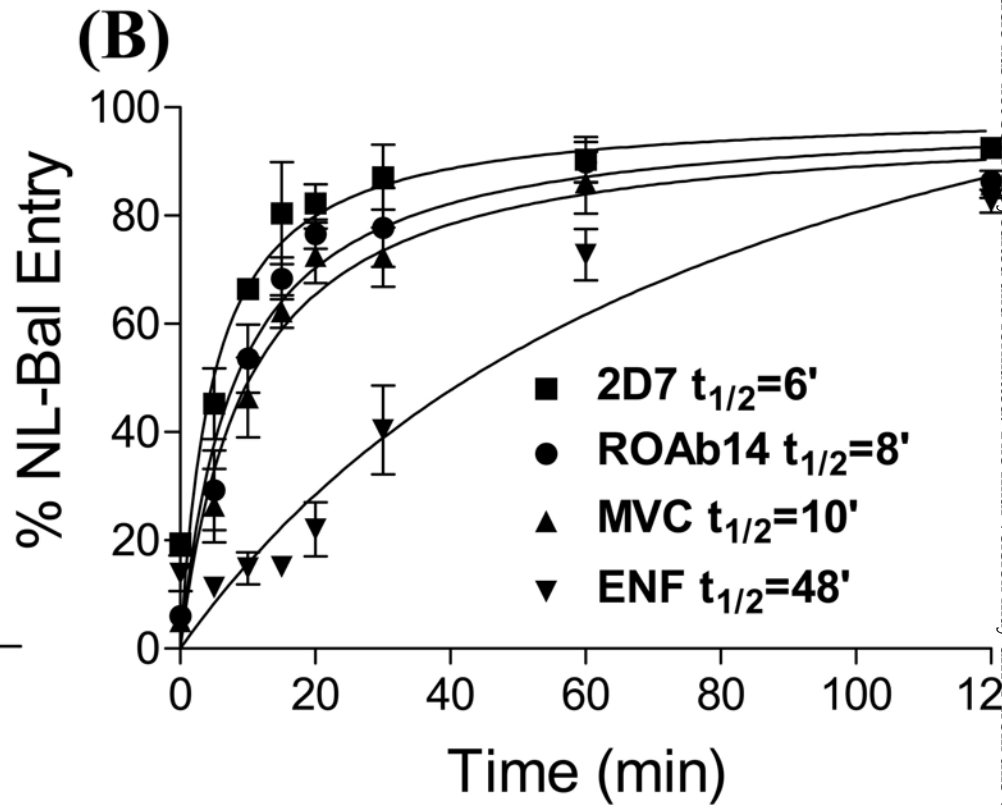

Figure 6

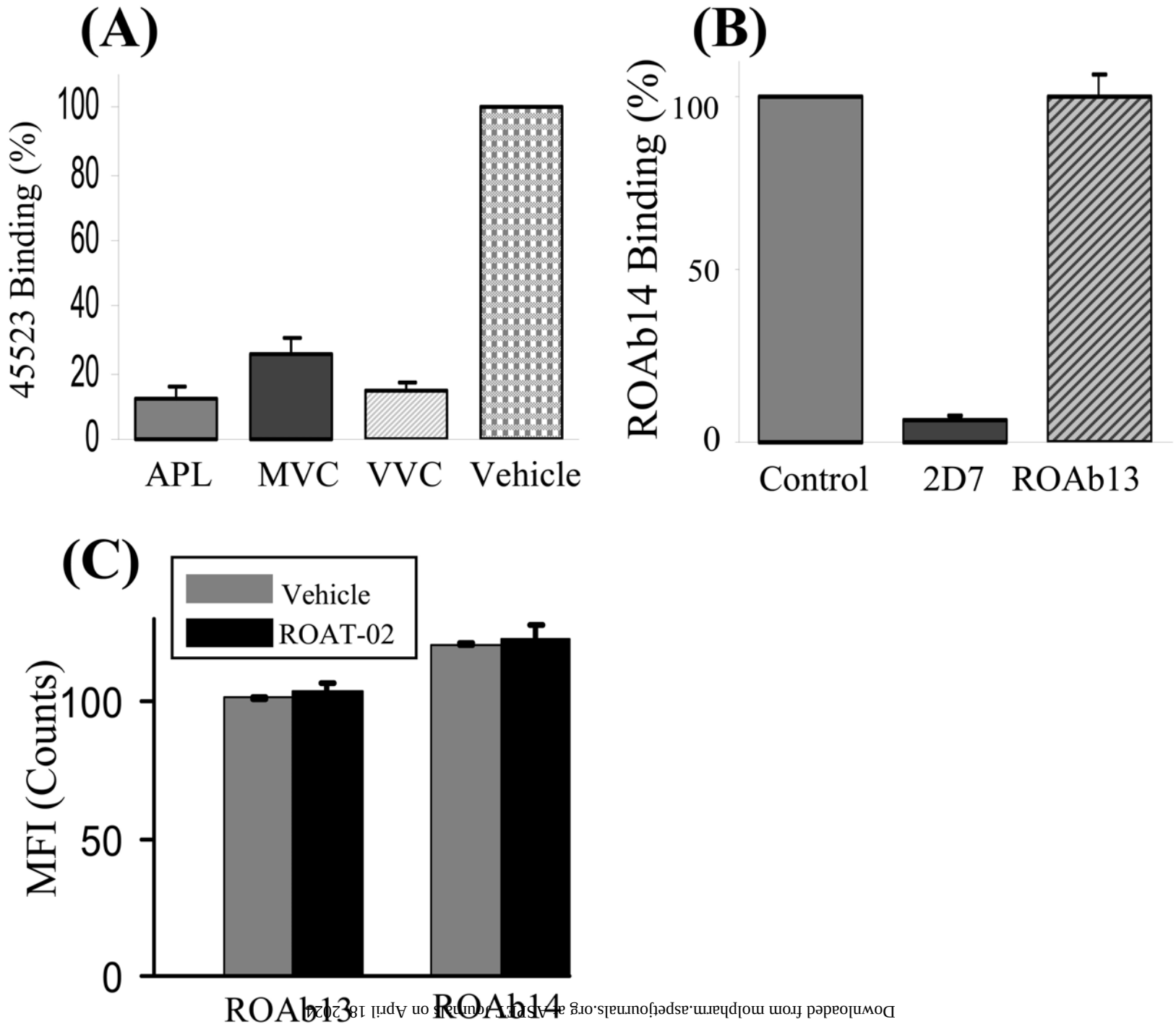

Molecular Pharmacology Fast Forward. Published on March 28, 2007 as DOI: 10.1124/mol.107.035055
This article has not been copyedited and formatted. The final version may differ from this version.

Figure 7

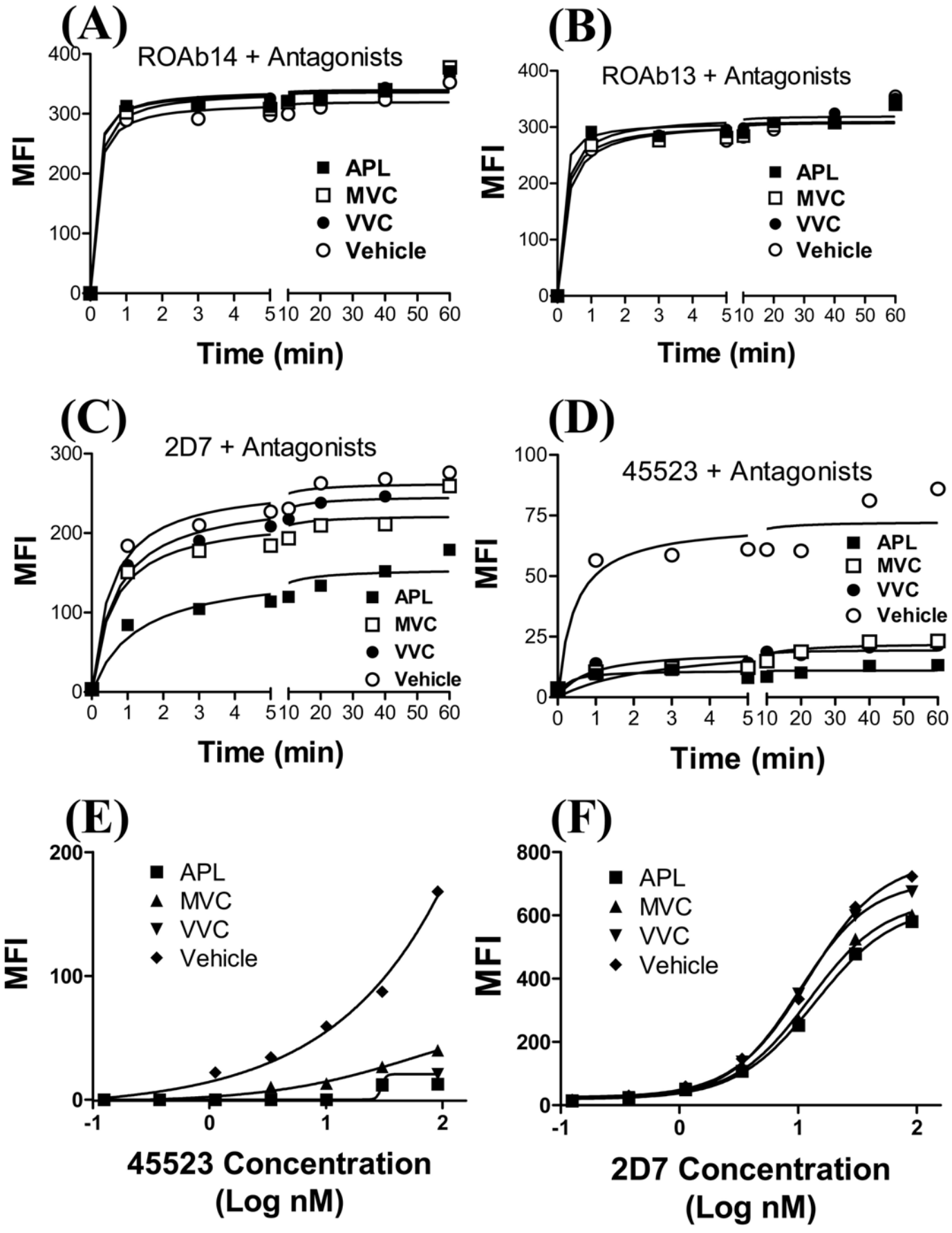

Figure 8

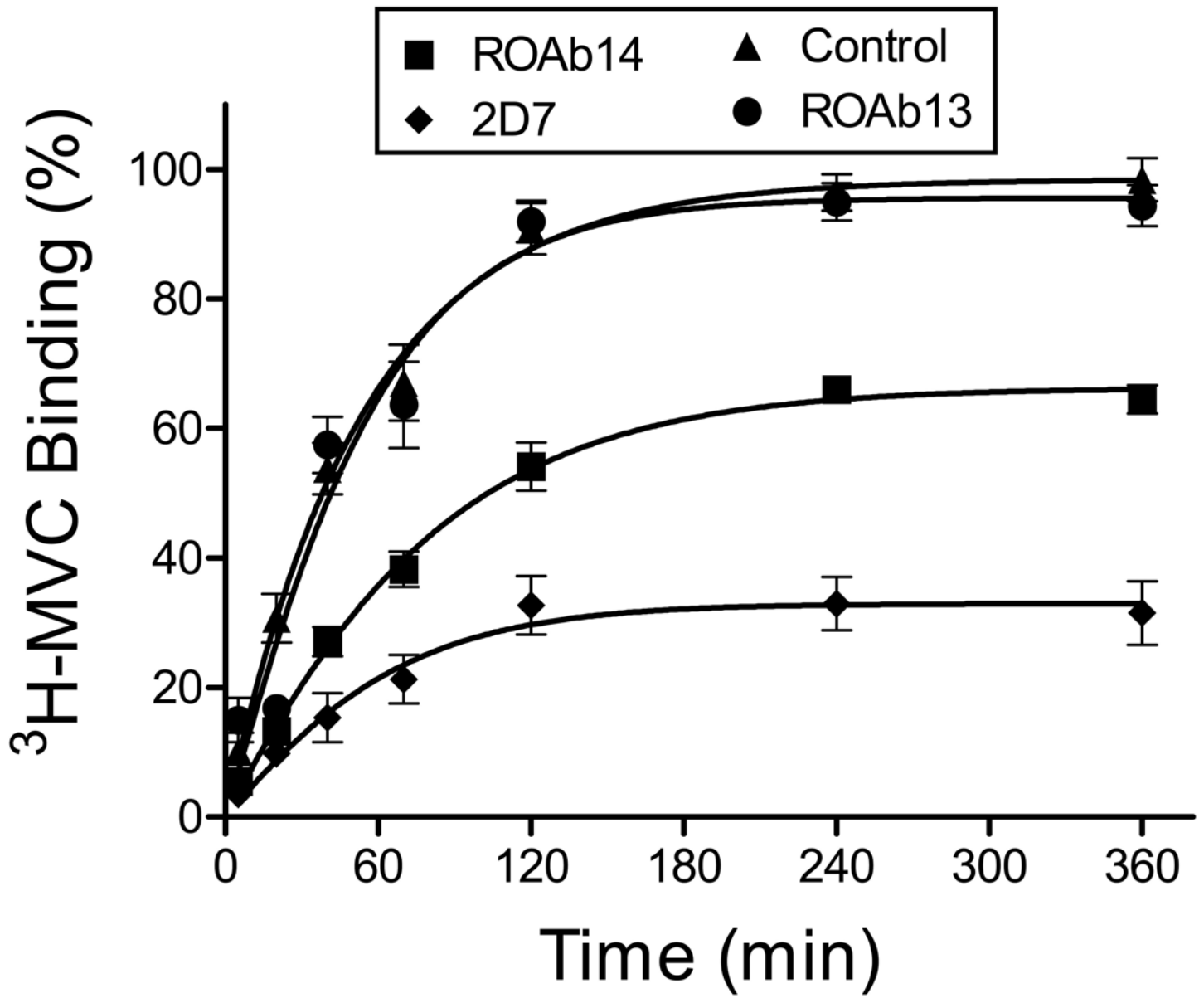

Figure 9